

UNIVERSIDADE DE SÃO PAULO

**INSTITUTO DE FÍSICA
CAIXA POSTAL 20516
01498-970 SÃO PAULO - SP
BRASIL**

PUBLICAÇÕES

IFUSP/P-1043

**RELATIVISTIC HYDRODYNAMICS WITH QHD-I
EQUATION OF STATE**

D.P. Menezes

**Depto. de Física, Universidade Federal de Santa Catarina
Caixa Postal 476, 88049 Florianópolis, Brazil**

F.S. Navarra, M. Nielsen

Instituto de Física, Universidade de São Paulo

U. Ornik

**Gesellschaft für Schwerionenforschung,
Planckstr. 1, 6100 Darmstadt, Germany**

Março/1993

RELATIVISTIC HYDRODYNAMICS WITH QHD-I EQUATION OF STATE

D.P. MENEZES

Departamento de Física, Universidade Federal de Santa Catarina,
Caixa Postal 476, 88049 Florianópolis, Brazil

F.S. NAVARRA, M. NIELSEN

Nuclear Theory and Elementary Particle Phenomenology Group
Instituto de Física da Universidade de São Paulo,
Caixa Postal 20516, 01498-970 São Paulo, Brazil

U. ORNIK

Gesellschaft für Schwerionenforschung, Planckstr.1, 6100 Darmstadt, Germany

Abstract: We derive the equation of state of the QHD-I lagrangian in a classical approach. The obtained equation of state is then used as input in a relativistic hydrodynamical numerical routine. Rapidity and transverse momentum distributions are calculated and compared with experimental data on heavy ion collisions obtained at BNL-AGS and CERN-SPS.

1. INTRODUCTION

The interpretation of future data from heavy-ion experiments with the advent of ultrarelativistic heavy-ion colliders, such as the proposed Relativistic Heavy Ion Collider, presents a great challenge. An exciting possibility is that a quark-gluon plasma can be created in the laboratory, so that the transition between hadronic and subhadronic degrees of freedom can be studied. While the physics of the quark-gluon plasma is being studied in the framework of finite temperature QCD, techniques to study the hadronic phase using QCD directly are very limited at present and theoretical progress has been slow. Therefore, the knowledge of the hadronic matter equation of state (EOS) at temperatures and densities far from those encountered in ordinary nuclei is an important theoretical problem.

The description of the hadronic matter equation of state based on hadronic degrees of freedom is very attractive. First of all because hadrons are the particles observed experimentally and are also the most efficient variables at low densities and temperatures. Second because extreme conditions can be extrapolated from calibrations made between hadronic calculations and observed hadron-hadron scattering and empirical nuclear properties. Finally because an accurate hadronic description is required to isolate and identify true signatures of the QCD behavior in nuclear matter.

Information about the equation of state can be extracted from experimental data. At high energies the main observables are the final particles rapidity and transverse momentum distributions. The most frequently used equations of state are those of the pionic ideal gas, mesonic resonances ideal gas, quark-gluon ideal gas and combinations of these three including a first or second order phase transition between hadronic and quark-gluon phases. As expected those EOS containing quarks and gluons involve more degrees of freedom and therefore have more entropy than the others and they lead to

higher rapidity distributions and consequently a larger number of produced particles with less kinetic energy. A systematic study of the effects of the equation of state on the observables can be found in ref. [1]. A problem with all these equations of state is that they do not include baryons. Their applicability relies on the assumption that the thermal system which generates the final particles has approximately zero baryon number. This is however strongly contradicted by experimental data.

In this work we use a relativistic quantum field theory of mesons and baryons, which is known as quantum hadrodynamics (QHD-I) [2], to study heavy-ion collisions using hydrodynamic models. Calculations can then be compared to data to see if the framework is related to real world, and to decide where QHD-I succeeds and where it fails. We perform a calculation of finite-temperature nuclear matter properties in the mean-field approximation to the Walecka model. This model contains some basic elements of hadronic theories of nuclei, namely, baryons coupled strongly to neutral scalar and vector fields, and is known to describe quite well the saturation of nuclear matter and static properties of nuclei [2]. Recently it was extended [3] to finite temperatures and its equation of state (EOS) was derived. This EOS correctly incorporates baryon-meson interactions and thus is adequate to describe the properties of hot and dense baryon-rich matter formed in relativistic heavy-ion collisions. The inclusion of baryons in the EOS in a dynamically consistent way as done in ref. [3] is not only more realistic but a necessary step before claiming, as it was already done, that only an EOS with a QCD phase is able to correctly describe experimental data.

The only way to test an EOS is to hydrodynamically study its temporal evolution and compare the final state particle distributions with experimental data. In this paper we use the QHD-I EOS as input for the HYLANDER¹ hydrodynamical numerical code [4]. We calculate proton, pion and negatively charged particles rapidity and

¹Hydrodynamical LANDau Expansion Routine.

transverse momentum distributions and compare them with data obtained by the BNL-AGS E802 and CERN-SPS NA35 collaborations.

In the next section we derive the EOS. Section 3 contains information about hydrodynamics such as initial conditions and freeze-out. Section 4 is devoted to results and comparison with data, and finally in section 5 are the conclusions.

2. THE EQUATION OF STATE

Our starting point is the standard QHD-I lagrangian density

$$\mathcal{L} = \bar{\Psi}[\gamma_\mu(i\partial^\mu - g_v V^\mu) - (M - g_s \phi)]\Psi + \frac{1}{2}(\partial_\mu \phi \partial^\mu \phi - m_s^2 \phi^2) - \frac{1}{4}F_{\mu\nu}F^{\mu\nu} + \frac{1}{2}m_v^2 V_\mu V^\mu, \quad (2.1)$$

where $F_{\mu\nu} = \partial_\mu V_\nu - \partial_\nu V_\mu$.

In what follows we derive the equation of state for this lagrangian in the nuclear matter rest frame. The resulting equations are the same as obtained in ref. [3] (eqs. (3.44) to (3.47) of ref. [3]) except for small differences due to a different choice of frame. We present here the derivation of the EOS because the method used is different and, in some aspects, simpler. Introducing the canonically conjugated fields we write the hamiltonian of the model as

$$H = \int d^3x \Psi^\dagger [\alpha \cdot (\mathbf{p} - g_v \mathbf{V}) + \beta(M - g_s \phi) + g_v V^0] \Psi + \frac{1}{2} \int d^3x (\Pi_\phi^2 + \nabla \phi \cdot \nabla \phi + m_s^2 \phi^2) + \frac{1}{2} \int d^3x [\Pi_{V_i}^2 - 2\Pi_{V_i} \partial_i V^0 + \nabla V_i \cdot \nabla V_i - \partial_j V_i \partial_i V_j + m_v^2 (\mathbf{V}^2 - V^{0^2})]. \quad (2.2)$$

In a classical approximation the energy of such system (in the nuclear case) with particles at the position \mathbf{r} , instant t with momentum \mathbf{p} described by the distribution function $f_+(\mathbf{r}, \mathbf{p}, t)$ and anti-particles at the position \mathbf{r} , instant t with momentum $-\mathbf{p}$ described by the distribution function $f_-(\mathbf{r}, \mathbf{p}, t)$, is

$$E = 4 \int \frac{d^3r d^3p}{(2\pi)^3} (f_+(\mathbf{r}, \mathbf{p}, t) h_+ - f_-(\mathbf{r}, \mathbf{p}, t) h_-) + \frac{1}{2} \int d^3r (\Pi_\Phi^2 + \nabla\Phi \cdot \nabla\Phi + m_s^2 \Phi^2) + \frac{1}{2} \int d^3r [\Pi_V^2 - 2\Pi_V \partial_i V^0 + \nabla V^i \cdot \nabla V^i - \partial_j V^i \partial_i V^j + m_v^2 (V^2 - V^{02})], \quad (2.3)$$

where h_+ (h_-) is the one-body hamiltonian for particles (anti-particles):

$$h_\pm(\mathbf{r}, \mathbf{p}, t) = \pm \sqrt{(\mathbf{p} - g_v \mathbf{V})^2 + (M - g_s \Phi)^2} + g_v V^0. \quad (2.4)$$

The parameters of the model are given in ref. [3], i.e., $C_s^2 = g_s^2 (M^2/m_s^2) = 357.4$, $C_v^2 = g_v^2 (M^2/m_v^2) = 273.8$, and produce a zero-temperature equilibrium at $k_F = 1.30 \text{ fm}^{-1}$, with a binding energy of 15.75 MeV and a compressibility of $K = 545 \text{ MeV}$. This compressibility is quite large and smaller values could be obtained with the introduction of scalar meson self interactions [5].

The equations describing the time evolution of the fields Φ and V^μ are derived from Hamilton's equations and are

$$\frac{\partial^2 \Phi}{\partial t^2} - \nabla^2 \Phi + m_s^2 \Phi = g_s \rho_s(\mathbf{r}, t), \quad (2.5a)$$

$$\frac{\partial^2 V^0}{\partial t^2} - \nabla^2 V^0 + m_v^2 V^0 = g_v \rho(\mathbf{r}, t) + \frac{\partial}{\partial t} \left(\frac{\partial V^0}{\partial t} + \nabla \cdot \mathbf{V} \right), \quad (2.5b)$$

$$\frac{\partial^2 V^i}{\partial t^2} - \nabla^2 V^i + m_v^2 V^i = g_v j^i(\mathbf{r}, t) + \frac{\partial}{\partial x^i} \left(\frac{\partial V^0}{\partial t} + \nabla \cdot \mathbf{V} \right), \quad (2.5c)$$

where the baryonic density is given by

$$\rho_B(\mathbf{r}, t) = 4 \int \frac{d^3p}{(2\pi)^3} (f_+(\mathbf{r}, \mathbf{p}, t) - f_-(\mathbf{r}, \mathbf{p}, t)), \quad (2.6a)$$

while the nuclear scalar and current density are expressed by

$$\rho_s(\mathbf{r}, t) = 4 \int \frac{d^3p}{(2\pi)^3} \frac{M^*}{\epsilon^*} (f_+(\mathbf{r}, \mathbf{p}, t) + f_-(\mathbf{r}, \mathbf{p}, t)), \quad (2.6b)$$

and

$$\mathbf{J}(\mathbf{r}, t) = 4 \int \frac{d^3p}{(2\pi)^3} \frac{\mathbf{p}^*}{\epsilon^*} (f_+(\mathbf{r}, \mathbf{p}, t) + f_-(\mathbf{r}, \mathbf{p}, t)) \quad (2.6c)$$

respectively. In eqs. (2.6b and c) $M^* = M - g_s \Phi$, $\mathbf{p}^* = \mathbf{p} - g_v \mathbf{V}$ and $\epsilon^* = \sqrt{\mathbf{p}^{*2} + M^{*2}}$.

In the mean field approximation the meson field operators are replaced by their expectation values which are constant fields. The equations of motion become simply

$$m_s^2 \Phi = g_s \rho_s, \quad (2.7a)$$

$$m_v^2 V_0 = g_v \rho_B, \quad (2.7b)$$

$$m_v^2 \mathbf{V} = g_v \mathbf{J}. \quad (2.7c)$$

From eq. (2.6a) we can see that the number of particles and the number of anti-particles is not separately conserved. However, their difference, the baryonic number

$$N_B = 4\mathcal{V} \int \frac{d^3p}{(2\pi)^3} (f_+ - f_-)$$

is conserved.

The classical entropy of a gas of fermions and anti-fermions is [6]

$$S = \frac{S}{\mathcal{V}} = -4 \int \frac{d^3p}{(2\pi)^3} \left(f_+ \ln \left(\frac{f_+}{1 - f_+} \right) + \ln(1 - f_+) + f_- \ln \left(\frac{f_-}{1 - f_-} \right) + \ln(1 - f_-) \right), \quad (2.8)$$

where \mathcal{V} is the volume of the system.

The thermodynamic potential is defined as

$$\Omega = E - TS - \mu_B N_B = -P\mathcal{V}, \quad (2.9)$$

where μ_B is the chemical potential, T is the temperature and P is the pressure.

For a system in equilibrium, the distribution functions should be chosen to make the thermodynamic potential Ω stationary. We get

$$f_\pm(\mathbf{p}) = \frac{1}{1 + \exp[(\epsilon^* \mp \nu)/T]}, \quad (2.10)$$

with $\nu = \mu_B - g_v V^0$ being the effective chemical potential. We notice that f_\pm is a function of ϵ^* , therefore eq. (2.7c) gives $\mathbf{J} = 0$ and $\mathbf{V} = 0$.

The equation of state in its final form can be written as

$$\frac{E}{V} = \mathcal{E} = 4 \int \frac{d^3p}{(2\pi)^3} (f_+ + f_-) \epsilon^* + \frac{m_s^2}{2g_s^2} (M - M^*)^2 + \frac{g_v^2}{2m_v^2} \rho_B^2, \quad (2.11a)$$

$$S = \frac{1}{T} \left(4 \int \frac{d^3p}{(2\pi)^3} (f_+ + f_-) \epsilon^* + \frac{4}{3} \int \frac{d^3p}{(2\pi)^3} (f_+ + f_-) \frac{p^2}{\epsilon^*} + \frac{g_v^2}{2m_v^2} \rho_B^2 - \mu_B \rho_B \right), \quad (2.11b)$$

$$P = \frac{4}{3} \int \frac{d^3p}{(2\pi)^3} (f_+ + f_-) \frac{p^2}{\epsilon^*} - \frac{m_s^2}{2g_s^2} (M - M^*)^2 + \frac{g_v^2}{2m_v^2} \rho_B^2, \quad (2.11c)$$

$$\rho_B = 4 \int \frac{d^3p}{(2\pi)^3} (f_+ - f_-), \quad (2.11d)$$

$$M^* = M - \frac{4g_s^2}{m_s^2} \int \frac{d^3p}{(2\pi)^3} (f_+ + f_-) \frac{M^*}{\epsilon^*}. \quad (2.11e)$$

Note that $(f_+ + f_-)$ enters in eq. (2.11e) and $(f_+ - f_-)$ enters in eq. (2.11d). The different signs in these expressions imply that there can be a finite, self-consistent shift in mass $M \rightarrow M^*$ at zero baryon density ($\nu = 0$) as the temperature T is increased, due to the baryon anti-baryon pairs formation.

To compute the thermodynamic functions, one first chooses T and ν and solves the self-consistency condition (2.11e) to determine M^* . At low temperature, there may be several solutions for M^* for fixed T and ν [2,3]. These values of M^* , ν and T specify f_+ and f_- through eq. (2.10) and can then be used to compute the remaining integrals in eqs. (2.11).

3. THE HYDRODYNAMIC EVOLUTION

In the hydrodynamical picture of a heavy-ion reaction one can divide the evolution of the system into three stages: first there is a compression and thermalization of nuclear matter, then this highly excited fireball begins to expand according to the laws of relativistic hydrodynamics and finally the system decouples and particles are emitted. Here we use Landau-type initial conditions. The system is assumed to be

partially stopped and its energy is deposited homogeneously in a cylindrical initial volume, the longitudinal size of which is Lorentz-contracted by the factor

$$\gamma = K \frac{E_p}{m}, \quad (3.1)$$

where E_p is the projectile energy in the equal-velocity-frame and m its mass. K is the inelasticity factor, varying between zero and one and being the fraction of the total reaction energy which is effectively thermalized and available for particle production. It is defined as

$$K = M_T / \sqrt{s}, \quad (3.2)$$

where M_T is the invariant mass of the thermalized system and \sqrt{s} is the total invariant reaction energy.

Because only a fraction of all nucleons is really participating in the reaction, we multiply the total baryon number of the system by a factor K_b which is about 0.85 in the CERN NA35 experiment and 0.9 in the BNL-AGS E802 experiment.

Given K and K_b , the initial size, energy and baryon number of the fireball are fixed. These are all the initial conditions which are required for the hydrodynamical expansion. In order to know any other thermodynamical quantity the EOS is needed.

After specifying the initial conditions the nuclear matter is treated as an ideal relativistic fluid obeying the laws of hydrodynamics which are written in a brief form as follows

$$\partial_\mu T^{\mu\nu} = 0, \quad (3.3)$$

$$\partial_\mu B^\mu = 0, \quad (3.4)$$

$$T^{\mu\nu} = (\mathcal{E} + P) u^\mu u^\nu - P g^{\mu\nu}, \quad (3.5)$$

$$B^\mu = \rho_B u^\mu, \quad (3.6)$$

where P , \mathcal{E} and ρ_B are the pressure, energy density and baryon density defined in the last section. u^μ is the four-velocity and $g^{\mu\nu}$ is the metric tensor. This coupled system of partial differential equations, together with the relation between \mathcal{E} and P given by the EOS, is solved numerically in 3+1 dimensions by the program HYLANDER. The hydrodynamical description ends when a critical “freeze-out” temperature T_f is reached. It is assumed that at temperatures lower than T_f the mean distance between the fluid constituents exceeds the range of nuclear interaction. The freeze out temperature was first estimated by Landau [7] to be of the order of the pion mass ($T_f = 0.139$ GeV) which is also the value used in this work. A discussion on freeze-out criteria can be found in refs. [8] and [9]. When a fluid point reaches the temperature T_f its space-time coordinates and 4-velocity components are stored. At the end of the expansion we obtain a collection of space-time points which form the freeze-out hypersurface.

During the freeze-out stage the final particles are emitted from the fireball. The transition from the fluid description to the free particle stage is a complicated process. Here we use a simple model for it. We assume that the fluid freezes out into “stable” π 's, K 's, nucleons and Λ 's. By stable we mean that the decay of the particle or resonance occurs after the complete freeze-out of the system. The resonance contribution we take into account by the introduction of a chemical potential for pions μ_R which describes the overpopulation of pions due to the decoupling of resonances [10]. This procedure seems to be a good approximation of the full treatment of final state interactions [4] which is very computer time consuming. At this point one might ask how can we talk about pions and kaons when our original lagrangian does not contain these degrees of freedom. The answer is that, in the spirit of all hydrodynamical models, we do not treat the microscopic processes through which the particles (pions, kaons, etc.) are created. The final particles are instead statistically produced according to an energy partition process. The initial degrees of freedom generate the equation of state (which

is then used in the solution of the equations of hydrodynamics) and are not directly related to the final degrees of freedom.

The system of frozen out particles we describe by a decoupling temperature T_f , a chemical potential for baryons and strange particles and a chemical potential for pions.

The chemical potentials depend on the conserved charges Q^k of the system. For strongly interacting particles the charges can be the baryon number B^k and the strangeness S^k of a particle i . We will use the following abbreviation to express the general chemical potential $\tilde{\mu}_i$ acting on a subset of particles of type i

$$\tilde{\mu}_i = \sum_k Q_i^k \mu^k. \quad (3.7)$$

They are determined by the requirement that the energy density ε_{fl} and the baryonic density $\rho_B^{(fl)}$ of the fluid equals that of the frozen out particles and that there is local thermal and chemical equilibrium at freeze-out. The net strangeness is assumed to be zero. We obtain the following system of equations:

$$\mathcal{E}_{fl}(T) = \mathcal{E}_\pi^{therm}(\tilde{\mu}_R, T) + \mathcal{E}_K(\tilde{\mu}_S, T) + \mathcal{E}_N(\tilde{\mu}_B, T) + \mathcal{E}_\Lambda(\tilde{\mu}_\Lambda, T) \quad (3.8)$$

$$\rho_B^{(fl)}(T) = \sum_k B_k n_k(\tilde{\mu}_k, T) \quad (3.9)$$

$$s_{fl}(T) = \sum_k S_k n_k(\tilde{\mu}_k, T) = 0 \quad (3.10)$$

where

$$\mathcal{E}_i(\tilde{\mu}_i^k, T) = \frac{g_i}{2\pi^2} \int p^2 dp \frac{E_i}{\exp\left(\frac{E_i - \tilde{\mu}_i}{T}\right) \pm 1} \quad (3.11)$$

$$n_i(\tilde{\mu}_i^k, T) = \frac{g_i}{2\pi^2} \int p^2 dp \frac{1}{\exp\left(\frac{E_i - \tilde{\mu}_i}{T}\right) \pm 1} \quad (3.12)$$

The coupled system of nonlinear equations (3.8)–(3.12) can be solved and we obtain from the fluid variables ε_{fl} , $\rho_B^{(fl)}$ and $s_{fl} = 0$, the quantities μ_R , μ_S , μ_B which determine the free particle state after freeze-out.

With the information of the chemical potential the single inclusive distribution functions of a particle i emitted from a hydrodynamically expanding source with a four-velocity field u^μ on a hypersurface σ is given by collecting all space-time points of temperature T_f to a hypersurface σ in Minkowski-space [11]

$$E_i \frac{d^3n}{dp_i^3} = \frac{g_i}{(2\pi)^3} \int_{\sigma} \frac{p_i^\mu d\sigma_\mu}{\exp[(p_i^\mu u_\mu - \tilde{\mu}_i)/T_f] \pm 1}, \quad (3.13)$$

where g_i denotes the degeneracy-factor of the particle and the sign in the denominator of the integrand depends on whether one deals with bosons or fermions. $d\sigma_\mu$ is the surface element with four-velocity u^μ .

4. NUMERICAL RESULTS

Integrating eq. (3.13) we obtain rapidity and transverse momentum distributions which can be compared to experimental data.

In Fig. 1 we compare our rapidity distributions of protons and negative pions with those measured by the E802 collaboration at the BNL-AGS for central $Si-AI$ collisions with $E_{lab} = 14.5A$ GeV [12]. We have chosen this target-projectile combination just because it is a nearly symmetric system and the numerical calculations could be easier performed. As it can be seen we reproduce the proton spectrum fairly well whereas the pion distribution is underpredicted by a factor four. This behavior was qualitatively expected in our approach. At these energies quite few baryon anti-baryon pairs are produced and the observed protons come mostly from the original nuclei. The imposition of baryon number conservation ensures that our total proton yield be very close to the measured one. As for the shape our curve shows a dip in the very central rapidity region and a large tail indicating that we have too much kinetic energy. The small number of produced pions indicates that our EOS has too low entropy. This is not

surprising since the QHD-I lagrangian contains a small number of degrees of freedom. Although we might still have some freedom to change the value of the parameters, a serious attempt to fit data (which might still contain uncertainties in pion and proton yields of order of 30%) is beyond the scope of this work.

In Fig. 2 we compare our rapidity distributions of negative charged particles and protons with those measured by the NA35 collaboration at the CERN-SPS for $S-S$ collisions with $E_{lab} = 200A$ GeV [13,14]. Again we underpredict the charged particle yield. The proton rapidity distribution reproduces the two-bumps structure of data but the position of the bumps is wrong by one unit in rapidity. In our calculations the baryonic matter was initially at rest. This might be a reasonable assumption at lower (AGS) energies, but at increasing energies nuclear transparency becomes more and more important so that even the participant baryons (which are initially captured in the collision volume and finally found in central rapidity region) do have initial longitudinal velocity. With an initial rapidity distribution for baryons, data can be correctly reproduced (as was shown in ref. [15]). As for the total proton yield CERN data excluded the protons originating from the decay of Λ particles. Our calculations do not include this subtraction process since we are not considering final state interactions. The inclusion of this effect would probably lower the curve and make the total proton yield smaller than the experimental one. At SPS energies baryon production is more intense than at AGS. This feature will not be well described by the QHD-I EOS because of its low entropy.

In Fig. 3 we show the corresponding transverse momentum distributions. Fig. 3a and 3b show the transverse momentum spectra of negatively charged secondaries of different rapidity intervals. As it can be seen we overestimate the large p_T tail and underestimate the low p_T part of the spectrum. This seems to be a common feature of all hydrodynamical calculations as long as they ignore the enhanced contribution of

mesons with increasing energy of the fireball. The transverse momentum distribution of protons, shown in Fig. 3c, is consistent with their rapidity distribution, showing that we obtain protons which are too fast in the transverse direction and too slow in the longitudinal direction. Here again the introduction of an initial velocity field and the use of an entropy-rich EOS would make agreement with data much better.

5. CONCLUSIONS

This work can be regarded as a continuation of ref. [3]. The equation of state of QHD-I was derived in an alternative way and used as input in a realistic hydrodynamical calculation. Rapidity and transverse momentum distributions were calculated and compared with experimental data on heavy-ion collisions obtained at AGS and SPS. The main qualitative features of data could be reproduced but a very precise description of data could not be achieved. If our calculations had produced irreparably wrong results we would have started to believe that quark-gluon degrees of freedom, either in the form of strings or as a quark-gluon gas, were indispensable. However, this was not the case and it might be possible to remain alive with hadronic degrees of freedom even at CERN energies.

In order to improve our hadronic-based description we clearly need more entropy in our EOS, i.e., more degrees of freedom. A simple way to check whether this is correct is to repeat our calculations using an EOS which is an ideal gas of many baryons, mesons and respective resonances not dynamically connected, i.e., not derived from a lagrangian. Preliminary calculations [16] show indeed that this EOS generates pion rapidity distributions which are already very close to data. Naively one would then try to include all these degrees of freedom in the lagrangian. This produces however no entropy increase as long as one keeps the mean-field approximation as it was done here.

In order to circumvent this difficult one might try to replace our crude approximation by a mean-field expansion, allowing for the actual evaluation of corrections to the simplest mean-field approximation. This approach has been used successfully in a different context by L.C. Yong and A.F.R. de Toledo Piza [17].

ACKNOWLEDGEMENTS

This work was partially supported by FAPESP – Brazil, CNPq – Brazil and the Los Alamos National Laboratory and the Deutsche Forschungsgemeinschaft. Udo Ornik acknowledges a post doctoral DFG fellowship. We are indebted to D. Strottman for instructive discussions.

REFERENCES

- [1] U. Ornik, "Relativistische Hydrodynamik mit Phasenübergang in der Kosmologie und in Kern-Kern Stößen", Ph.D. Thesis, Marburg (1990).
- [2] B.D. Serot and J. D. Walecka, *Adv. Nucl. Phys.* **16**, 1 (1986).
- [3] R.J. Furnstahl and B.D. Serot, *Phys. Rev.* **C41**, 262 (1990).
- [4] U. Ornik and R.M. Weiner, *Phys. Lett.* **B263**, 503 (1991), and references therein.
- [5] J. Boguta and A.R. Bordmer, *Nucl. Phys.* **A292**, 413 (1977).
- [6] L.D. Landau and E.M. Lifshitz, "Statistical Physics", part 1 (Oxford: Pergamon) 3rd. edn. (1980).
- [7] L.D. Landau, *Izv. Akad. Nauk. SSSR* **17**, 51 (1953).
- [8] F.S. Navarra et al., *Phys. Rev.* **C45**, 2552 (1992).
- [9] K.S. Lee, U. Heinz and E. Schnedermann, *Z. Phys.* **C48**, 525 (1990).
- [10] P. Gerber, H. Leutwyler and J.L. Goity, *Phys. Lett.* **B246**, 513 (1990).
- [11] F. Cooper and G. Frye *Phys. Rev.* **D10**, 186 (1974).
- [12] M.C. Sarabura, Ph.D. Thesis, MIT, 1989.
- [13] S. Wenig, Ph.D. Thesis, GSI-Report 90-23, October 1990.
- [14] NA35-collaboration and Bartke et al., *Z. Phys.* **C48**, 191 (1990).
- [15] J. Bolz, U. Ornik and R.M. Weiner, *Phys. Rev.* **C46**, 2047 (1992).
- [16] U. Ornik and D. Strottman, in preparation.
- [17] L.C. Yong and A.F.R. de Toledo Piza, *Mod. Phys. Lett.* **A5**, 1605 (1990).

FIGURE CAPTIONS

- Fig. 1. a) Rapidity distribution of protons in a $^{28}\text{Si}+^{27}\text{Al}$ collision at $E_{lab} = 14.6A$ GeV. Data points come from the E802 collaboration, ref. [5], and the solid line is our calculation. b) the same as a) for negative pions.
- Fig. 2. a) Rapidity distribution of negatively charged particles in a $^{32}\text{S}+^{32}\text{S}$ collision at $E_{lab} = 200A$ GeV. Data points come from the NA35 collaboration, ref. [6] and [7], and the solid line is our calculation. b) the same as a) for protons.
- Fig. 3. a) Transverse momentum distribution of negatively charged particles measured in the same experiment as in Fig. 2. Points are the NA35 data and the solid line is our calculation. b) the same as in a) for a different rapidity interval. c) the same as in a) for protons in the full rapidity space.

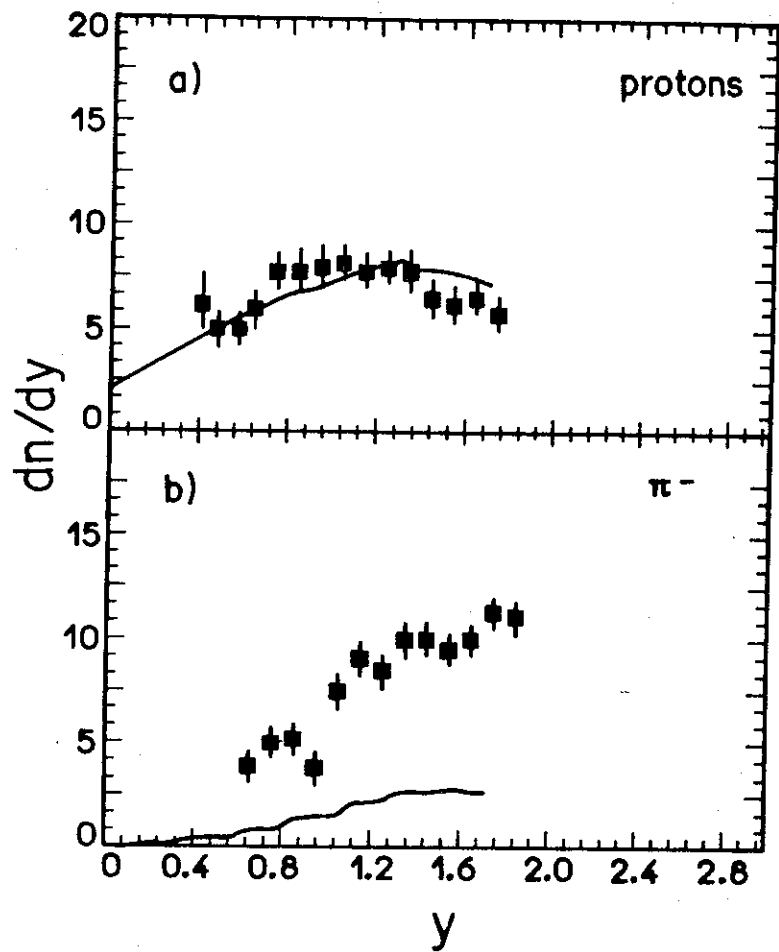


FIG. 1

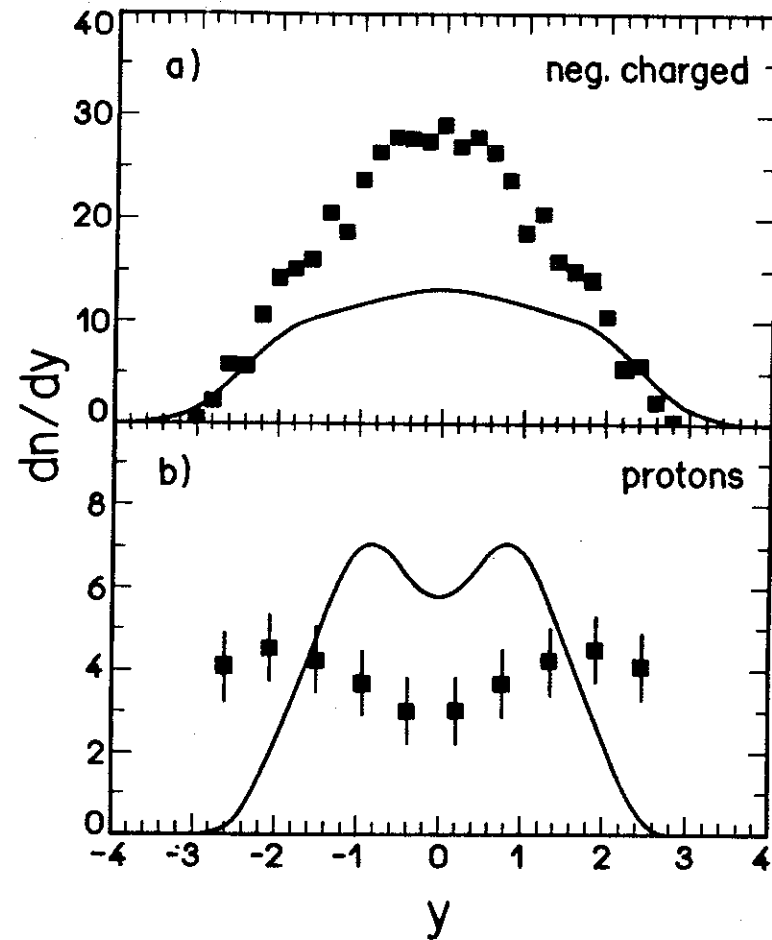


FIG. 2

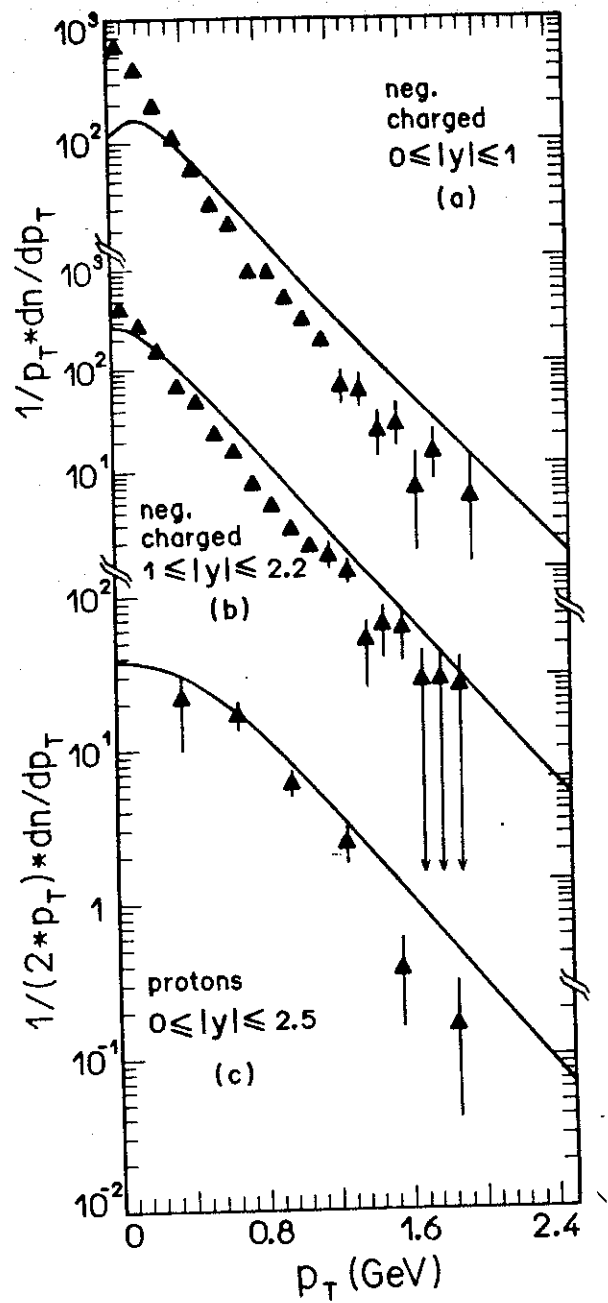


FIG. 3